Supporting Information

Reddy et al. 10.1073/pnas.0910665107

SI Experimental Procedures

Tissue Harvest and Analysis. Mammary glands and tumors were removed and either fixed in 10% buffered formalin overnight at 4 °C, frozen in frozen section medium (Neg-50, Richard-Allan Scientific) on dry ice, or snap-frozen in liquid nitrogen. Formalin-fixed tissues were paraffin embedded, and 3-μm sections were placed on slides for immunostaining. Sections (10 μm) were generated from frozen tissue blocks and placed on slides. Immunohistochemistry and immunofluorescence were performed as described previously (1). Briefly, formalin-fixed paraffin sections were deparaffinized, rehydrated, and subjected to antigen retrieval in 10 mM sodium citrate, pH 6.0. Frozen sections were fixed in 4% paraformaldehyde and permeabilized in 0.1% Triton-X before staining. The manufacturer's protocol for the MOM, Vectastain Elite ABC Rabbit, or Rat kits (Vector Labs; cat no. PK-2200, PK-6101, PK-6104) was then followed. Western blotting was performed as described previously (2, 3).

Antibodies. Primary antibodies used in these experiments include rabbit antibodies against PyMT (Calbiochem, DP10L), phospho-S10 Histone H3 (Upstate, 06–570), p53 (Novocastra, CM5p), Ki67 (Novocastra, Ki67p), p-S15-p53 (Cell Signaling, 9284), β-actin (Cell Signaling, 4970), p16 (Santa Cruz, sc-1207), DcR2 (Stressgen, AAP-371), and 53BP1 (Bethyl, A300-273A); mouse monoclonal antibodies against GFP (BD Biosciences, 632281), HA (Covance, MMS-101P), γH2AX (Upstate, 05–636), and p-S1981-ATM (Rockland, 200–301-500); and a rat ARF antibody (Abcam, ab26696).

TUNEL and SA-β-Gal Staining. For TUNEL staining, paraffin sections were treated identically as above but without antigen retrieval, and the manufacturer's protocol for the Apoptag Red *In Situ* TUNEL detection kit (Chemicon, S7165) was followed. SA-β-Gal staining was performed on 10-μm mammary gland or mammary tumor cryosections either using a SA-β-Gal activity kit (Cell Signaling, 9860) or a method described previously (4, 5). For SA-β-Gal/Ki67 double-staining, standard immunohistochemistry for Ki67 was performed on frozen sections immediately on the completion of SA-β-Gal staining.

Microscopy. All brightfield images were captured at 40× using a Leica DMLB microscope. Fluorescent images were either captured at 40× with a ZeissAxioskop 2 plus microscope or at 63× or 100× with a Zeiss/Applied Precision SoftWoRx Image Restoration Microscope and processed using SoftWoRx deconvolution software.

Expression Analysis. RNA was extracted from mouse tissue using the RNAeasy kit (Qiagen). The following probe sets were used for qRT-PCR analysis: *p53* (Mm01731287_m1), *Mdm2* (Mm01233136_m1), *p21* (Mm1303209_m1), and *18s* (Hs99999901_s1) (Applied Biosystems).

Statistical Analysis. All images shown are representative of at least 10 fields viewed over two stained sections per animal. Quantitation was performed using a minimum of three random fields per animal. All columns represent mean ± SEM. All statistical analyses were performed using Student's *t* test unless otherwise indicated.

1. Du Z, et al. (2006) Introduction of oncogenes into mammary glands in vivo with an avian retroviral vector initiates and promotes carcinogenesis in mouse models. *Proc Natl Acad Sci USA* 103:17396–17401.
2. Li Y, et al. (2001) Deficiency of Pten accelerates mammary oncogenesis in MMTV-Wnt-1 transgenic mice. *BioMed Central Mol Biol* 2:2.
3. Li Y, et al. (2003) Evidence that transgenes encoding components of the Wnt signaling pathway preferentially induce mammary cancers from progenitor cells. *Proc Natl Acad Sci USA* 100:15853–15858.
4. Dimri GP, et al. (1995) A biomarker that identifies senescent human cells in culture and in aging skin in vivo. *Proc Natl Acad Sci USA* 92:9363–9367.
5. Bandyopadhyay D, Gatza C, Donehower LA, Medrano EE (2005) Analysis of cellular senescence in culture in vivo: The senescence-associated beta-galactosidase assay. *Curr Protoc Cell Biol* 27:18.9.1–18.9.9.

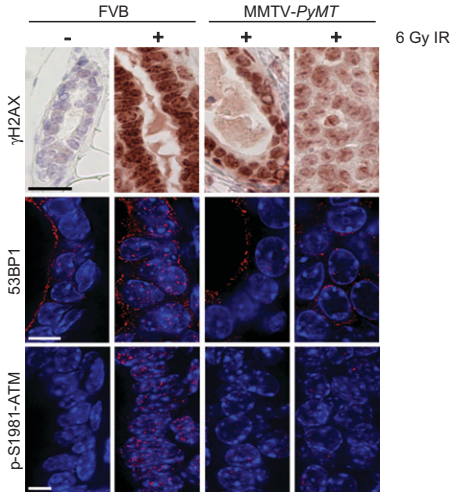

Fig. S1. Poor DDR induction in MMTV-*PyMT* transgenic mice. γH2AX, 53BP1, and p-S1981-ATM staining of mammary glands from 8-week-old nontransgenic (n = 3) or MMTV-*PyMT* transgenic mice (n = 3). Where indicated, mice were exposed to 6 Gy IR and killed 30 min later. Brightfield images are 40× with 20 μm scale bar. Deconvolution immunofluorescent images are 100× (53BP1) or 60× (p-S1981-ATM) with 5-μm scale bar.

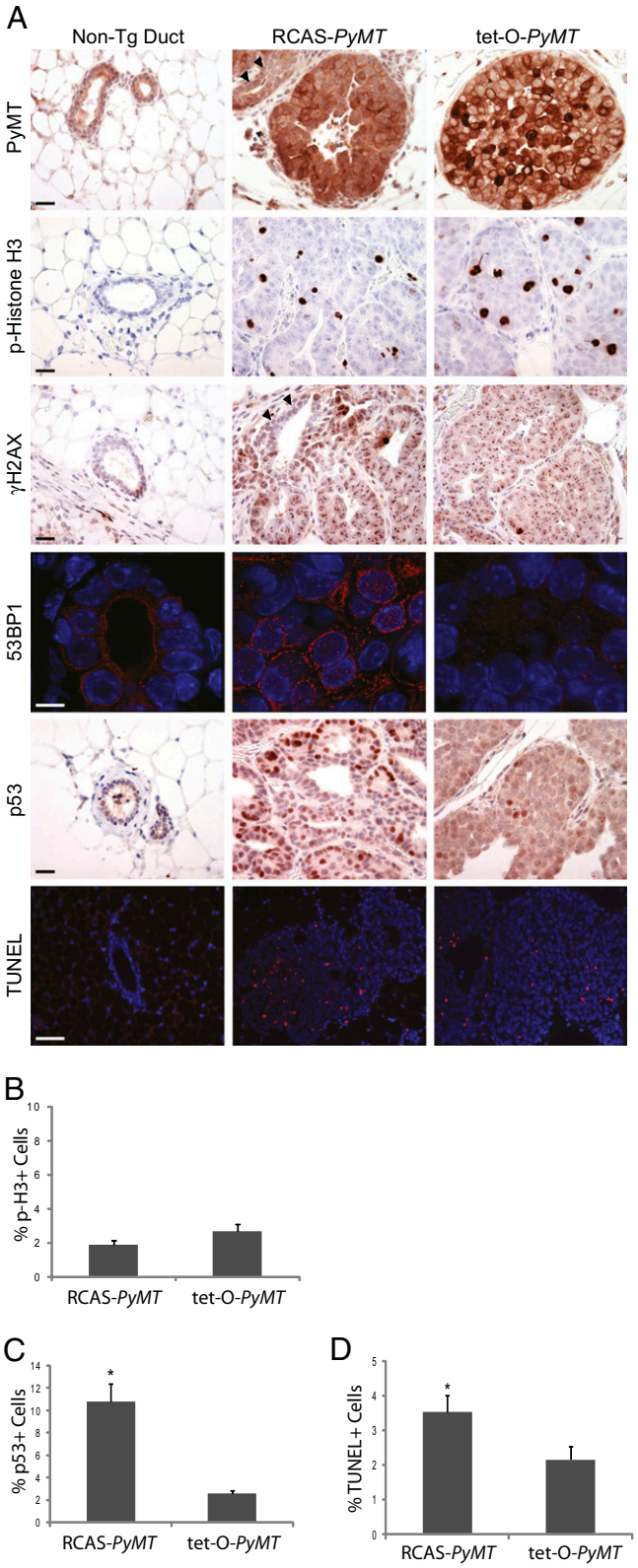

Fig. S2. Somatic activation of PyMT oncogenic signaling induces a robust DDR in mouse mammary glands. (*A*) RCAS-*PyMT* ($n = 4$) and MMTV-*rtTA*/tet-O-*PyMT-IRES-Luc* mammary hyperplasias ($n = 3$) as well as nontransgenic ducts from 7-week-old mice were stained by immunohistochemistry or immunofluorescence for the proteins indicated at the right or by TUNEL. Arrowheads indicate adjacent normal mammary epithelium included as a comparison with RCAS-*PyMT* early lesions. Brightfield images are 40× with 20 μm scale bar. 53BP1 deconvolution immunofluorescent images are 100× with 5-μm scale bar. TUNEL immunofluorescent images are 40× with 20-μm scale bar. (*B–D*) Percentages of phospho-histone H3-positive nuclei (*B*), p53-positive nuclei (*C*), and TUNEL-positive cells (*D*) in hyperplastic early lesions arising in 7-week-old RCAS-*PyMT* ($n = 4$) or MMTV-*rtTA*/tet-O-*PyMT-IRES-Luc* ($n = 3$) mice. Columns represent mean ± SEM. *$P = 0.01–0.05$.

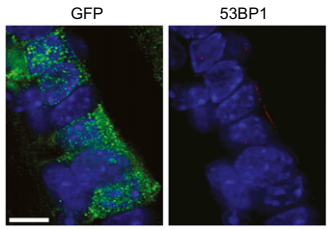

Fig. S3. RCAS-*GFP* viral infection does not induce a DDR. Representative 53BP1 and GFP co-immunofluorescence in RCAS-*GFP*–infected cells in mammary glands from 12-week-old MMTV-*tva* mice (n = 5). Deconvolution immunofluorescent images are 63× with 5-μm scale bar.

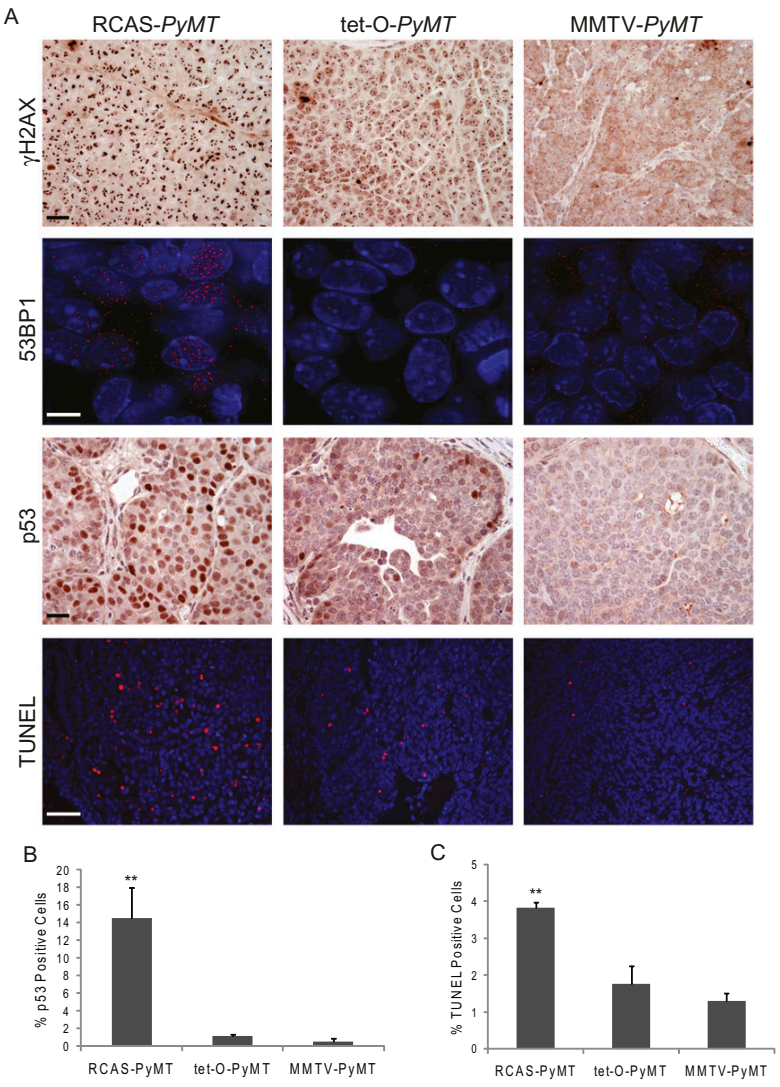

Fig. S4. A DDR persists in RCAS-*PyMT*-induced tumors. (*A*) Mammary tumors induced by RCAS-*PyMT* (*n* = 4), MMTV-*rtTA*/tet-O-*PyMT-IRES-Luc* (*n* = 4), or MMTV-*PyMT* (*n* = 3) were stained by immunohistochemistry or immunofluorescence for the proteins indicated or by TUNEL. Brightfield images are 40× with 20-μm scale bar. 53BP1 deconvolution immunofluorescent images are ×100 with 5-μm scale bar. TUNEL immunofluorescent images are 40× with 20-μm scale bar. (*B* and *C*) Percentages of p53-positive nuclei (*B*) or TUNEL-positive cells (*C*) in tumors induced by RCAS-*PyMT* (*n* = 4), tet-O-*PyMT* (*n* = 3), or MMTV-*PyMT* (*n* = 3). Columns represent mean ± SEM. Statistical analysis was performed using univariate ANOVA. *, *P* = 0.01–0.05; **, *P* = 0.001–0.01.

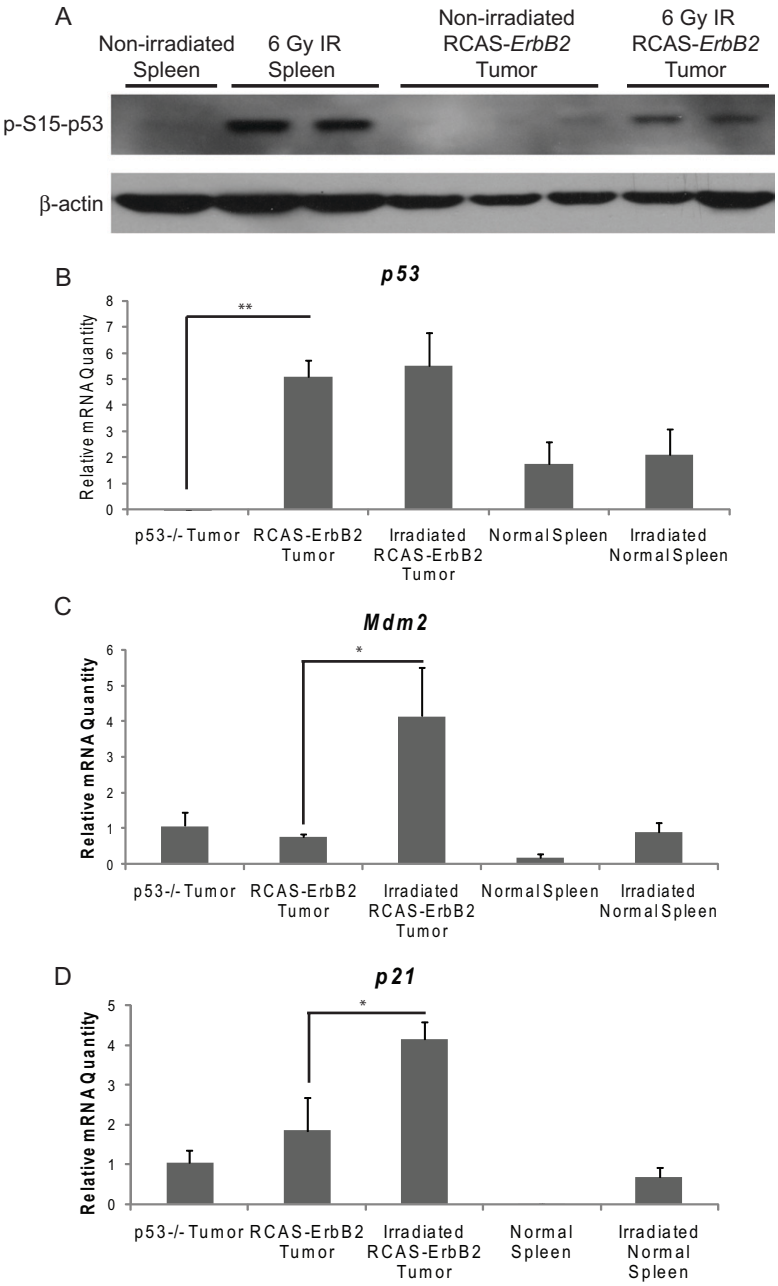

Fig. S5. *p53* remains intact and can be rendered functional in RCAS-*ErbB2*–induced mammary tumors. (*A*) Western blotting for phospho-S15-p53 in the tissues indicated at the top. β-actin immunoblotting was included as a loading control. Irradiated mice (6 Gy) were killed 6 h later for spleen or 16 h later for tumors. (*B* and *D*) qRT-PCR for the messages indicated. Samples tested include $p53^{-/-}$ mammary tumors ($n = 2$), nonirradiated ($n = 5$) and irradiated ($n = 3$) RCAS-*ErbB2*-induced mammary tumors, and both normal and irradiated splenic tissue ($n = 3$ for each). All samples were normalized to 18s RNA. *p53* was analyzed relative to normal spleen; p53 target genes, *Mdm2* and *p21,* were evaluated relative to $p53^{-/-}$ tumors that were also transgenic for MMTV-*Wnt-1*. Columns represent mean ± SEM. *, $P = 0.01–0.05$; **, $P = 0.001–0.01$.